Earth and Planetary Science Letters, 97 (1990) 332–352
Elsevier Science Publishers B.V., Amsterdam – Printed in The Netherlands

[KT]

^{210}Pb scavenging in the North Atlantic and North Pacific Oceans

J. Kirk Cochran [1], Thomas McKibbin-Vaughan [1], Mark M. Dornblaser [1,*], David Hirschberg [1], Hugh D. Livingston [2] and Ken O. Buesseler [2]

[1] *Marine Sciences Research Center, State University of New York, Stony Brook, NY 11794-5000 (U.S.A.)*
[2] *Woods Hole Oceanographic Institution Woods Hole, MA 02543 (U.S.A.)*

Received April 24, 1989; revised version accepted December 15, 1989

The radionuclide ^{210}Pb shows significant geographic variations in the extent of its removal from the open ocean water column. This "texture of scavenging" is defined by mapping: (1) the integrated deficiency of ^{210}Pb in the water column, relative to its supply from the atmosphere and from in situ decay of dissolved ^{226}Ra, and (2) inventories of excess ^{210}Pb in deep-sea sediments. The ratio of ^{210}Pb deficiency to its supply, termed the scavenging effectiveness, is ~ 20% in the North Equatorial Pacific and ~ 50% in the North Atlantic. This variation is related to the combined effects of uptake of ^{210}Pb onto sinking particles and lateral transport of ^{210}Pb to areas of more intense removal. Sediment inventories of excess ^{210}Pb, normalized to the ^{210}Pb deficiency in the overlying water column, permit evaluation of the relative importance of these effects. In the North Equatorial Pacific virtually all of the ^{210}Pb removed from the water column is present in the underlying sediments but in the mid-latitude North Atlantic, the sediments comprise only about 50% of the ^{210}Pb removed. The deficiencies of ^{210}Pb in the mid-latitude North Atlantic sediments south of 50°N are qualitatively offset by surpluses in high-latitude sediments north of 50°N. Higher primary productivity and new production in the surface waters of the high-latitude North Atlantic and North Equatorial Pacific, relative to the oligotrophic central North Atlantic, may account for the greater fluxes of ^{210}Pb to bottom sediments in those areas.

1. Introduction

Oceanic mass balances for chemical species are commonly constructed by comparing inputs via the atmosphere, rivers or hydrothermal sources with outputs such as incorporation in sediments. Such a procedure is often constrained by inherent uncertainties in the magnitudes of sources or sinks and seldom permits assessment of regional variations in supply or removal. The naturally occurring ^{238}U, ^{235}U and ^{232}Th decay series contain several tracers which are produced in the oceans from decay of parent nuclides dissolved in sea water. These tracers are well suited for the construction of mass balances because distributions of their radioactive parents are rather well known, permitting the regional variations in supply of the daughters to be mapped. ^{210}Pb (half-life = 22.3 yr) is one such radionuclide, produced principally from decay of its grandparent ^{226}Ra, but also added to the surface ocean from the atmosphere.

The residence time of ^{210}Pb with respect to scavenging is short in the surface ocean, of the order of 1 year, while in the deep ocean the value is 30–100 years [1,2]. This relatively long residence time in the deep ocean permits ^{210}Pb to be transported from areas of low scavenging intensity to areas of more rapid removal. This pattern has been recognized through water column distributions [3–5] and through the identification of areas such as the west coast of the U.S.A. with greater-than-expected inventories of excess ^{210}Pb in bottom sediments [6,7]. Scavenging and transport in both the vertical and lateral sense affect the distribution of ^{210}Pb in the open ocean. The former includes uptake of ^{210}Pb onto suspended particles which can be aggregated as fecal pellets or marine snow and sink through the water column. The latter includes isopycnal transport of ^{210}Pb to areas of strong removal.

The vertical component of ^{210}Pb scavenging

* Present address: Ecosystems Center, Marine Biological Laboratory, Woods Hole, MA 02543, U.S.A.

0012-821X/90/$03.50

can be measured directly in the open ocean through measurements of ^{210}Pb in sediment trap material or inventories of excess ^{210}Pb in deep-sea sediments. Indeed, ^{210}Pb is commonly distributed through the upper 10 cm of deep-sea sediments by particle mixing by organisms and is a useful tracer to determine the rate of such mixing [8–15]. Under steady-state conditions, the inventory of excess ^{210}Pb ($^{210}Pb_{xs}$), or the integrated activity of ^{210}Pb unsupported by ^{226}Ra, in a deep-sea sediment core represents the flux of ^{210}Pb to the sea floor averaged over about 4–5 half-lives or 100 years. The flux required to support the inventory is obtained by multiplying by the decay constant for ^{210}Pb and represents the mean flux of ^{210}Pb to the seafloor. We note that the ^{210}Pb flux measured in near bottom sediment traps may not equal that derived from excess ^{210}Pb inventories in bottom sediments if scavenging of ^{210}Pb at the sediment–water interface is occurring [3,4,16]. However, Nozaki [16] has shown that scavenging at the seafloor is slow compared to mixing of water and that near-bottom ^{210}Pb profiles from the Pacific can be explained without enhanced scavenging at the sediment–water interface.

Removal of ^{210}Pb from the water column at any given site thus represents the combined effects of the vertical (diapycnal) and lateral (isopycnal) processes of scavenging and transport, and variation of the strengths of these processes from place to place defines the "texture" of ^{210}Pb scavenging in the open ocean. It is the goal of this paper to provide insight into the texture of ^{210}Pb scavenging by comparing the observed ^{210}Pb removal from the water column with fluxes measured in near-bottom sediment traps or calculated from sediment core data. If the ^{210}Pb flux measured in near-bottom sediment traps or calculated from excess ^{210}Pb inventories in underlying sediments equals the removal from the overlying water column, diapycnal processes must dominate the removal. If, on the other hand, ^{210}Pb removal from the water column is unequal to the flux to the underlying sediments, there must be import or export of ^{210}Pb from the area by lateral processes.

The data for comparison of water column removal and sediment inventories of ^{210}Pb are most complete for the North Atlantic and North Pacific Oceans and we focus our discussion on these areas.

2. Analytical methods

Some of the water column and sediment measurements of ^{210}Pb used here have been previously published, and analytical procedures are discussed in the primary references. We also present new water column data from the Northwest Atlantic Ocean (Table 3) and sediment data from the North Atlantic and North Pacific (Table 2, Appendix). Water samples were collected with 30 l Niskin bottles, often paired 10 m apart to provide sufficient sample for analysis of transuranic radionuclides [17]. The samples were promptly transferred to 60 l Delex containers, acidified to pH of 1–2 with HNO_3 and transported to the laboratory. Aliquots of 4 l were withdrawn from the 60 l samples for ^{210}Pb analysis. ^{208}Po or ^{209}Po yield tracers and 100 mg of Fe were added and NH_4OH was used to precipitate $Fe(OH)_3$ which carried the Po. The precipitate was dissolved in 1.5*N* HCl, ascorbic acid was added and Po was auto-plated onto silver disks. All samples were analyzed after at least one year of storage, and ^{210}Po and ^{210}Pb are presumed to be in equilibrium.

Sediment samples were collected using large area (generally 2500 cm^2) box cores from which subcores were taken. Sediment from the subcores was dried at 70°C for 24 h and ground to a powder. Samples of up to 1 g were totally dissolved in a mixture of HCl, HNO_3 and HF in the presence of ^{208}Po or ^{209}Po yield tracers. Following evaporation and dissolution in HCl, Po was plated in the same manner as the water samples. All samples were processed long enough after collection so that ^{210}Po and ^{210}Pb were in equilibrium. Following plating of Po, ^{226}Ra was determined on the sample solutions using the ^{222}Rn emanation method [35].

Some sediment samples also were analyzed by non-destructive gamma spectrometry using the 46.5 keV ^{210}Pb peak and the 352 keV ^{214}Pb peak for ^{226}Ra [18]. All sediment $^{210}Pb_{xs}$ data have been corrected to the time of collection of the core [10].

Sediment trap samples were collected at 1464 and 4832 m in the Nares Abyssal Plain. The 5-cup Oregon State University design was used, with sodium azide as a preservative [19]. Dried samples were analyzed for ^{210}Pb by the same procedure used for sediment samples.

3. Results and discussion

3.1. Water column and sediment ^{210}Pb data

Several sets of data are necessary to calculate the removal of ^{210}Pb from a given water column: (a) the dissolved ^{226}Ra profile; (b) the ^{210}Pb profile; and (c) the atmospheric flux of ^{210}Pb. The ^{226}Ra profile defines the in situ production of ^{210}Pb which, added to the atmospheric supply of ^{210}Pb, we refer to as the *total supply* of ^{210}Pb to a given water column. The integrated activity of ^{210}Pb present in the water column is subtracted from the total supply to get the water column ^{210}Pb deficiency or activity of ^{210}Pb removed from the water column.

The largest data set for both water column ^{226}Ra and ^{210}Pb is the GEOSECS data from the Atlantic, Pacific and Indian Oceans (summarized in [20]). The extent of data coverage for ^{210}Pb increased from the Atlantic to Pacific to Indian Ocean during the course of the GEOSECS program, while ^{226}Ra analyses were performed to about the same extent in the three oceans. For purposes of comparison with sediment ^{210}Pb data, this pattern is an unfortunate one in that the greatest sediment coverage is in the North Atlantic and North Equatorial Pacific.

An additional complication is that the water column ^{210}Pb data are not without analytical problems. In the Atlantic and Pacific, many of the ^{210}Pb analyses were made from samples collected with Gerard barrels. Bacon et al. [3] have shown that dissolved and particulate ^{210}Pb analyses made on Gerard samples taken in the Pacific often gave inconsistent results, with the particulate ^{210}Pb activity dominating the total activity in some cases. They ascribed this to the presence of quantities of rust which came from tools inadvertently dropped into the barrels. Under such circumstances, it is difficult to be confident of the measured ^{210}Pb values.

Additional measurements of ^{210}Pb in Pacific GEOSECS samples show similar problems. ^{210}Pb analyses were made on samples collected from

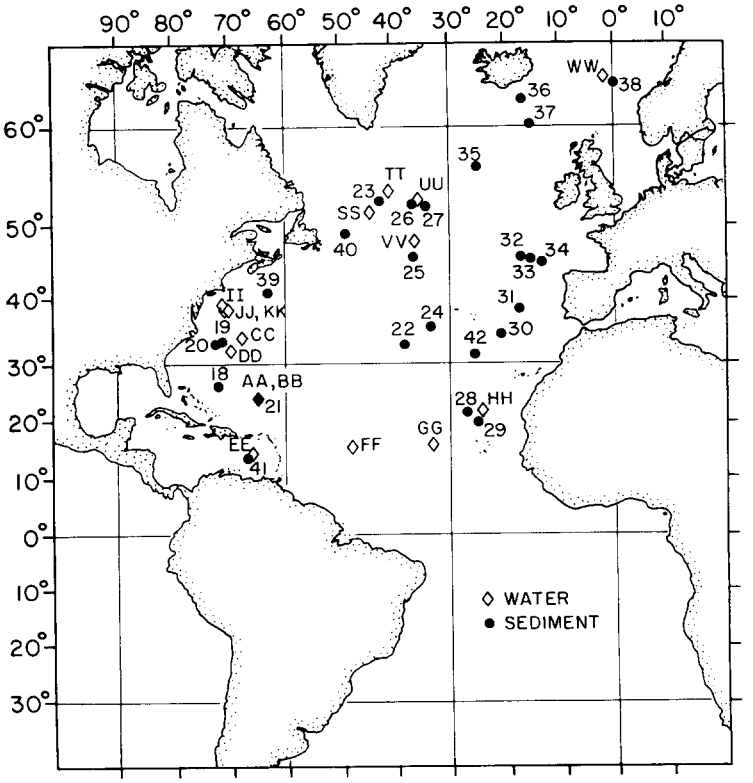

Fig. 1. North Atlantic water column stations and sediment core locations for which ^{210}Pb data are available. Letters and numbers refer to station code in Tables 1 and 2. Solid circles = sediment cores, open diamonds = water column stations.

Gerard barrels and also on library samples drawn from Niskin bottles. Comparison of the analyses of Gerard samples at Scripps Institution of Oceanography [21] with the filtered library samples from the same profile analyzed at Yale [22] shows that the former are commonly about 30% less than the latter [23]. Such a pattern could be produced by the same artifacts which affected the Atlantic samples as well as by uptake of ^{210}Pb on the walls of the Gerard barrels themselves. In general, we have used ^{210}Pb analyses of water collected in Niskin bottles to calculate ^{210}Pb removal from the water column [22–26,48, this study]. The only exception is the use of four stations taken by Bacon et al. [3] in the North Atlantic. The sample coverage is limited in this region, and the ^{210}Pb results from these samples are consistent with our new results for the Nares and Hatteras Abyssal Plains. For all the profiles, ^{226}Ra and ^{210}Pb inventories in units of dpm/cm^2 are calculated by interpolating the activities between the depths analyzed, multiplying by the depth interval and summing the results. The locations of all the water column stations used in the calculations are shown in Figs. 1 and 2.

The final component of the calculation of ^{210}Pb removal from the water column is the atmospheric flux. Turekian et al. [27] modeled this flux on the basis of estimated radon emanation rates from the continents, atmospheric circulation rates and aerosol mean residence times. Because of the prevailing west–east air circulation in the mid-latitudes, their model predicted that the atmospheric flux of ^{210}Pb to the ocean surface should decrease from west to east across the Pacific and Atlantic Oceans. Turekian et al. [27] also predicted that the ^{210}Pb fluxes would be lower in the southern hemisphere (15°–55°S) than in the northern hemisphere (15°–55°N) because of the greater integrated land area in the latter. However, measurements by Turekian et al. [28] show that the flux of ^{210}Pb in Bermuda (0.69 dpm/cm^2/yr) is comparable to that on the west coast of Great Britain (0.5 dpm/cm^2/yr, cited in [27]). In the

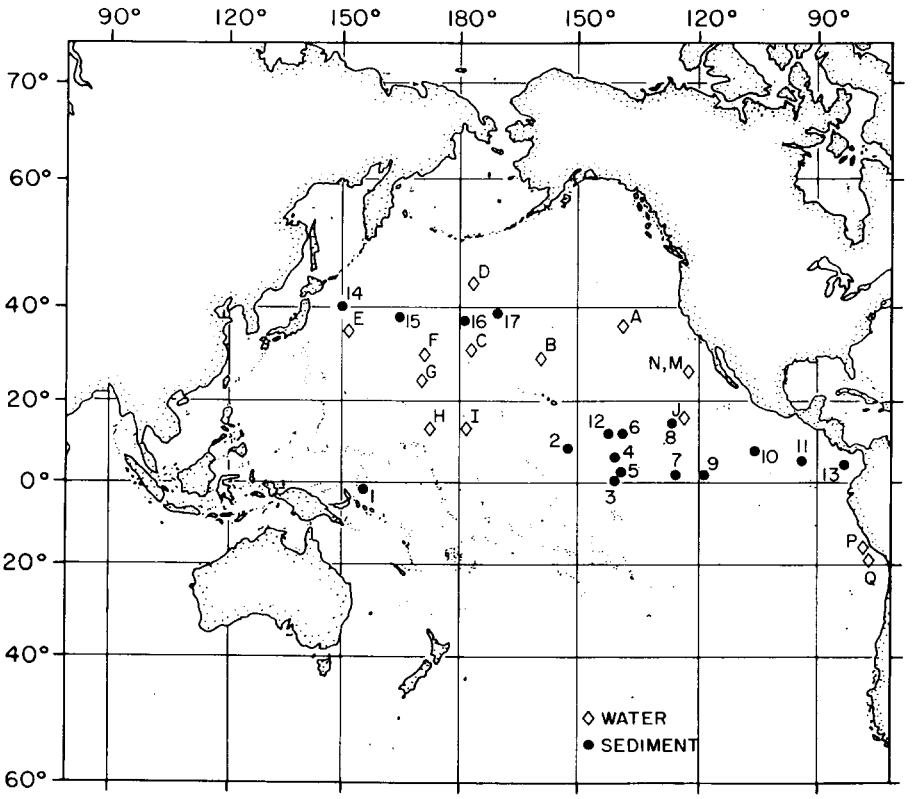

Fig. 2. North Pacific water column stations and sediment core locations for which ^{210}Pb data are available. Letters and numbers refer to station code in Tables 1 and 2. Solid circles = sediment cores, open diamonds = water column stations.

TABLE 1

Water column ^{210}Pb production, atmospheric supply and removal

Code	Station	Location	Water depth (m)	^{226}Ra inventory (dpm/cm^2)	Atmospheric ^{210}Pb (dpm/cm^2)	Total ^{210}Pb supply[a] (dpm/cm^2)	^{210}Pb inventory[b] (dpm/cm^2)	^{210}Pb deficiency[c] (dpm/cm^2)	Scavenging effectiveness[d] (%)	τ_{Scav} (y)
Pacific Ocean										
A	GEOSECS 202	36°6′N,139°34′W	5000	148[20]	8[29]	156	131[22]	25	16	170
B	212	30°0′N,159°50′W	5730	167[20]	8[29]	175	155[22]	20	11	260
C	214	32°1′N,176°59′W	5377	142[20]	8[29]	150	125[22]	25	17	160
D	217	44°36′N,176°50′W	6092	178[20]	8[29]	186	138[22]	48	26	91
E	223	34°58′N,151°50′E	6141	166[20]	8[29]	174	132[22]	42	24	100
F	226	30°34′N,170°38′E	5500	150[20]	8[29]	158	125[22]	33	21	120
G	227	24°59′N,170°5′E	5970	164[20]	8[29]	172	147[22]	25	15	180
H	229	12°53′N,173°28′E	5720	156[20]	8[29]	164	124[22]	40	24	100
I	231	14°6′N,178°38′W	5690	151[20]	8[29]	159	137[22]	22	14	200
J	343	16°31′N,122°59′W	4200	118[20]	8[29]	126	92[22]	34	27	87
M	347	28°30′N,121°29′W	4287	123[20]	8[29]	131	-	-	-	-
N	500	28°27′N,122°11′W	4145	-	8[29]	-	81[23]	50	38	52
P	Kn73-2-993	15°28′S,75°52′W	4000	115[e]	8[29]	123	57[48]	66	54	27
Q	Bartlett 3	18°58.9′S,74°58.7′W	4031	115[e]	8[29]	123	63[48]	60	49	33
Atlantic Ocean										
AA	TTO-NAS 24	23°17′N,64°9′W	5821	68[49]	22[28]	90	-	-	-	-
BB	NARES-1	23°13′N,64°8′W	5850	-	-	-	51[f]	39	43	42
CC	TTO-NAS 6	34°39′N,67°21′W	5220	58[49]	22[28]	80	-	-	-	-
DD	CMME 13	32°46′N,70°47′W	5400	-	-	-	43[f]	37	46	38
EE	Me-32-12	14.5°N,66°W	-	54[3]	22[28]	76	31[3]	45	59	22
FF	Me-32-18	15°N,48.5°W	-	43[3]	22[28]	65	34[3]	31	48	35
GG	Me-32-23	16.5°N,32°W	-	65[3]	16[27]	81	52[3]	29	36	57
HH	Me-32-27	21.5°N,24°W	-	66[3]	16[27]	82	54[3]	28	34	62
II	83-G-9 (Sta 4)	39°36′N,70°56′W	2351	25[e]	22[28]	47	15[45]	32	68	15
JJ	83-G-9 (Sta 5)	39°10′N,70°44′W	2804	29[e]	22[28]	51	17[45]	34	67	16
KK	83-G-9 (Sta 6)	38°38′N,70°15′W	3049	32[e]	22[28]	54	21[45]	33	61	20
SS	Kn51-665	51°10.5′N,43°40.0′W	3850	40[24]	10[24]	50	30[24]	20	40	48
TT	Kn51-670	53°40.0′N,40°00.8′W	3324	34[24]	10[24]	44	25[24]	19	43	42
UU	Kn51-677	52°41.7′N,35°28.3′W	3718	38[24]	10[24]	48	23[24]	25	52	30
VV	Kn51-681	47°45.5′N,35°47.0′W	4476	47[24]	10[24]	57	30[24]	27	47	36
WW	Kn54-6-70	63°50.0′N,0°51.8′E	2184	17[25]	10[24]	27	11[25]	16	59	22

[a] Calculated as the sum of ^{226}Ra inventory and atmospheric ^{210}Pb.

[b] Integrated ^{210}Pb activity in water column.

[c] Calculated as the difference between total ^{210}Pb supply and inventory.

[d] Calculated as ratio of ^{210}Pb deficiency to total ^{210}Pb supply $\times 100$.

[e] Values estimated from nearby stations.

[f] This study.

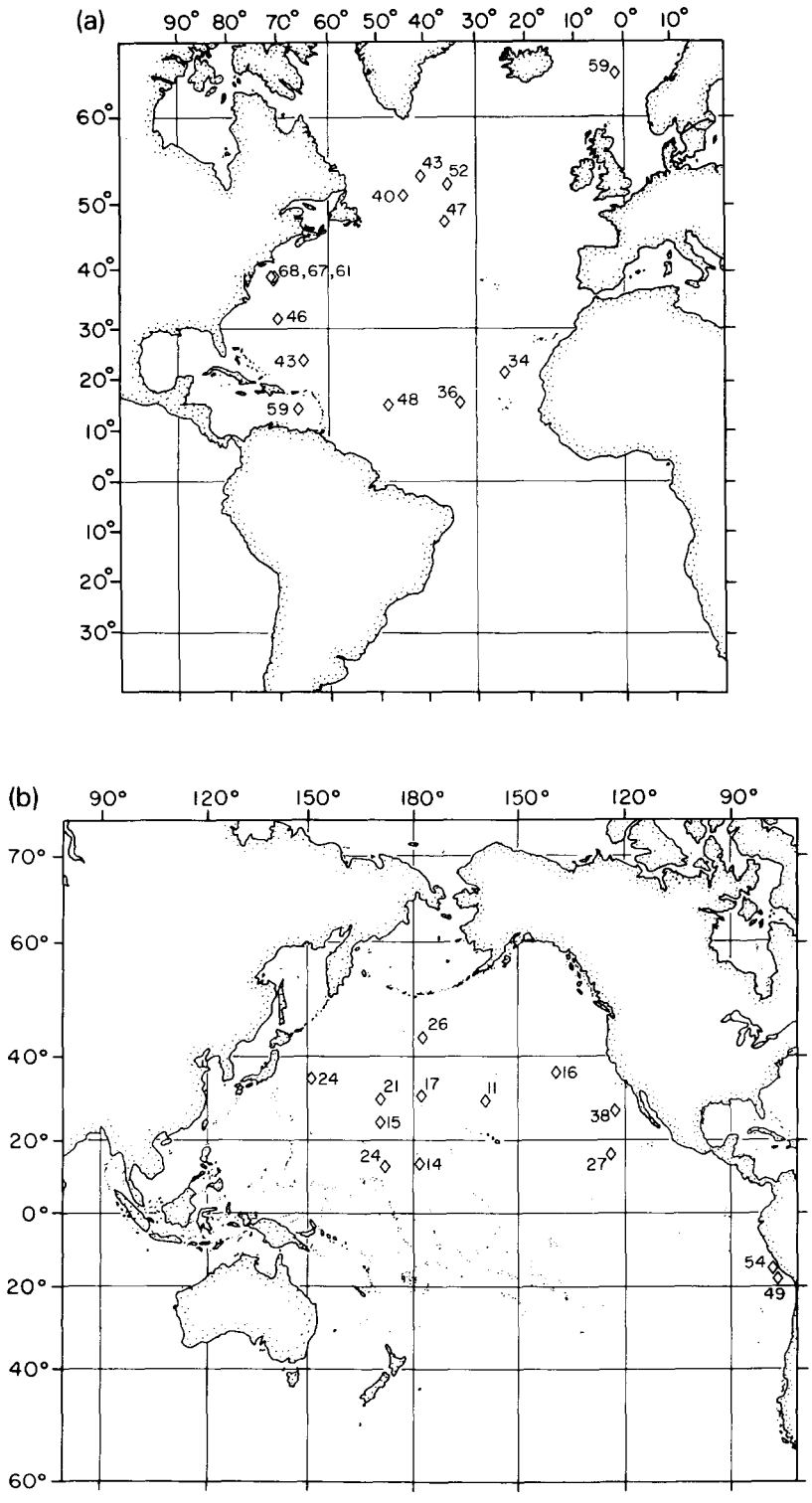

Fig. 3. Scavenging effectiveness for ^{210}Pb in: (a) the North Atlantic, and (b) the North Pacific Ocean. Maps are based on water column stations from Figs. 1 and 2. Scavenging effectiveness (calculated as %) is the water column ^{210}Pb deficiency normalized to the supply from the atmosphere and in situ decay of dissolved ^{226}Ra. See text for discussion.

Pacific, ^{210}Pb fluxes measured as part of the SEAREX program show a constant and relatively low value of 0.2-0.3 dpm/cm^2/yr throughout much of the North Pacific [29]. These patterns differ from the predictions of the Turekian et al. [27] model because continent-derived aerosols are scavenged from the boundary layer relatively close to the continental margin, and atmospheric deposition of ^{210}Pb in the open ocean is governed by supply of aerosols from the mid–upper troposhere to the marine boundary layer and from there, to the sea surface [29].

In the present study we use atmospheric fluxes measured in Bermuda (0.69 dpm/cm^2/yr; [28]) and Great Britain (0.5 dpm/cm^2/yr) for stations in the western and eastern North Atlantic respectively. The average value from the SEAREX dust network (0.25 dpm/cm^2/yr; [29]) is used for the North Equatorial Pacific. An intermediate value of 0.3 dpm/cm^2/yr calculated by Bacon et al. [24] is taken for the high-latitude North Atlantic.

Having assembled the relevant information, we calculate the total supply of ^{210}Pb to a given water column as the sum of the ^{226}Ra inventory and the standing crop of ^{210}Pb supported by the atmospheric flux. This sum represents the total ^{210}Pb available for scavenging, and values range from 27 to 186 dpm/cm^2 (Table 1). Subtracting the measured ^{210}Pb inventory in the water column from the total supply gives the water column ^{210}Pb deficiency. This value represents the activity of ^{210}Pb scavenged from the water column and ranges from 16 to 66 dpm/cm^2 (Table 1). Table 1 gives additional information on the stations and calculations.

Comparison of the water column ^{210}Pb deficiency at different sites requires normalizing the deficiency to the total ^{210}Pb supplied to the water column at that site. We term this ratio the "scavenging effectiveness" in that it describes how effectively ^{210}Pb is removed from the water column. Percentage values of scavenging effectiveness range from 11 to 68% (Fig. 3, Table 1). The concept of scavenging effectiveness (SE) is directly related to the residence time of ^{210}Pb with respect to scavenging, by equation (1):

$$\tau_{scav} = \left(\frac{1}{SE} - 1\right)\frac{1}{\lambda_{210}} \quad (1)$$

Values for τ_{scav} range from 15 to 260 yr (Table 1).

Inventories of excess ^{210}Pb in deep-sea sediments are calculated from measurements of ^{210}Pb

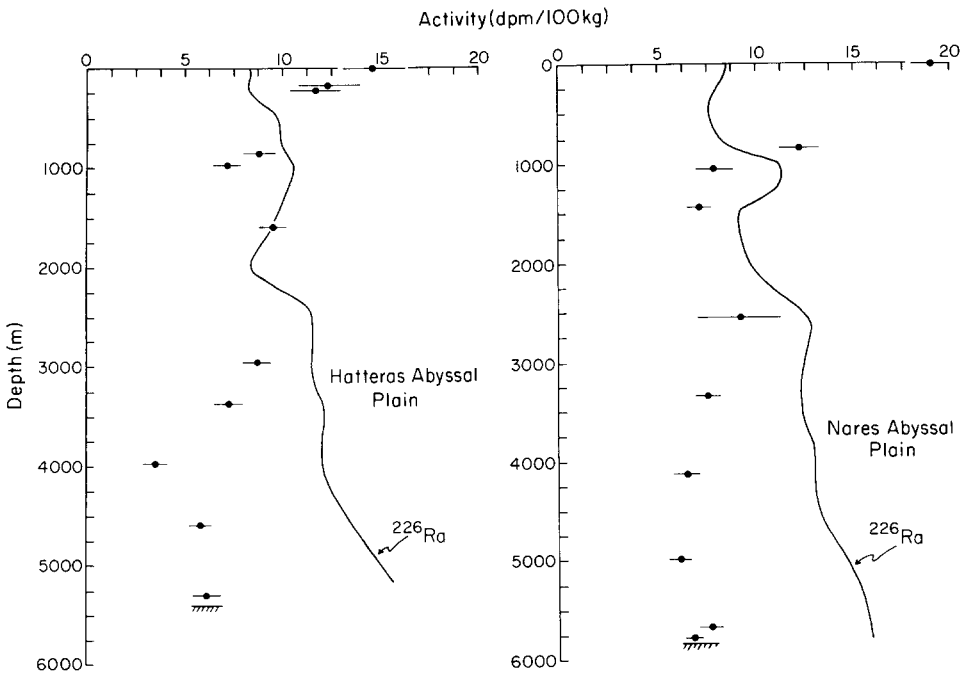

Fig. 4. Depth profiles of total ^{210}Pb (particulate and dissolved) (dpm/100 kg) at stations in the Nares and Hatteras Abyssal Plains of the Northwest Atlantic Ocean.

TABLE 2

Code	Core	Location	Water depth (m)	$^{210}Pb_{xs}$ inventory (dpm/cm^2)	Dry bulk density (g_{dry}/cm$^3_{wet}$)	Sediment type	Sediment accumulation rate (cm/ky)	Core type	Sediment inventory Water column deficiency	Reference
PACIFIC OCEAN (A-N)[d]										
1	ERDC-92BX	02°13.5'S,156°59.9'E	1598	11	0.60	carbonate	1.0-2.3	Box Core	.33	[9]
2	A47-16	09°02'N, 151°11'W	5050	35	0.25	siliceous	0.15	Box Core	1.06	[36]
3	58BX	00°N, 140°W	--	20	0.21-0.64	--	0.2	Box Core	.61	[50]
4	65BX	07°N, 140°W	--	11	0.08-0.21	--	0.2	Box Core	.33	"
5	MANOP Site C	01°N, 139°W	4450	26±5[a](n=5)	0.38-0.68	carbonate	--	Box Core, Lander	.79	[10],This Stud
6	B52-39	11°15'N, 139°04'W	4830	40	0.28	siliceous	0.30	Box Core	1.21	[36]
7	53BX	01°N, 125°W	--	31	0.05-0.29	--	--	Box Core	.94	[50]
8	C57-58	15°20'N, 125°54'W	4640	38	0.4	siliceous	0.14	Box Core	1.15	[36]
9	52BX	01°N, 118°W	--	38	0.03-0.45	--	--	Box Core	1.15	[50]
10	MANOP Site M	09°N, 104°W	3100	24±9[a](n=3)	0.16-0.30	metalliferous	--	Box Core, Lander	.73	[10]
11	MANOP Site H	06°30'N,92°50'W	3570	22±15[a](n=4)	0.10-0.26	hemipelagic	--	Box, Alvin, Lander Core	.67	[10],This Stud
12	MANOP Site S	11°N, 140°W	4900	23±28[a](n=3)	0.24-0.38	siliceous	--	Box Core, Lander	.70	"
13	PB81-2	05°20.7'N,81°56.2'W	3990	136	0.18-0.40	hemipelagic	2.3-3.8	Alvin Push Core	4.1	[51]
14	KH-80-2-5	40°00.2'N,150°00.0'E	5509	7	0.30	--	0.5	Tripod Core	.21	[52]
15	KH-80-2-6	39°02.5'N,166°00.3'E	5654	18	0.36	--	0.9	Tripod Core	.55	"
16	KH-80-2-8	38°03.3'N,179°45.7'W	5548	3	0.35	--	0.9	Tripod Core	.09	"
17	KH-80-2-9	39°00.0'N,170°00.8'W	5381	21	0.35	--	0.4	Tripod Core	.64	"
ATLANTIC OCEAN										
Northwest Atlantic (W of 40°W, S of 50°N; AA-DD[d])										
18	77G6-2	26°N, 73°W	5197	12[a]	0.58-0.74[b]	--	0.5-2.0	Box Core	.32	[11]
19	Hatteras Abyssal Plain	33°N,70'W	5300	20±6[a](n=7)	0.60[b]	lithogenous		Box Core	.53	[44]
20	77G6-4	32°N, 71°W	5200	14	0.66-0.85	--	0.5-2.0	Box Core	.37	[11]
21	Nares Abyssal Plain: 23°N,64°W		5750	9±4[a](n=8)	0.78	--		Box Core	.24	This Study
39	HEBBLE Site (Composite of 20 cores)	40°26.5'N,62°20.5'W	4820	67	.50-1.0	terrigenous clay	--	Box Core	1.8	[38]
Northeast Atlantic (E of 40°W, S of 50°N; FF,GG,HH,VV[d])										
25	KN51 Core 11	45°14.0'N,36°04.0'W	4189	30	0.60[b]	--	--	Gravity Core	1.0	This Study
28	76G4-11	21°N, 27°W	5032	12	0.80-0.93	--	0.5-2.0	Box Core	.41	[11]
29	76G4-10	20°N, 25°W	4660	12	0.82-0.95	--	0.5-2.0	Box Core	.41	"
30	CIR9/81 161	35°N, 20°30'W	5161	25	0.60[b]	--	1.8	Box Core	.86	[15]
31	CIR9/81 174	39°N, 17°W	5448	2	0.60[b]	--	0.8	Box Core	.07	"
32	Eastern North Atlantic I	46°N, 17°W	4760	10±1(n=2)	0.60[b]	--	2	Box Core	.34	[15]
33	Eastern North Atlantic II	46°N,16°W	4400	9±2(n=8)	0.60[b]	calcareous	2[c]	Box Core	.31	[14]
34	KN54 Core 15	45°36.5'N,12°34.3'W	4900	15	0.60[b]	--	--	Gravity Core	.52	This Study
42	Great Meteor East	31°N, 25°W	5400	17±5(n=5)	0.5	terrigenous/carbonate	0.5-1	Box Core	.59	[54]
Mid-ocean Ridge (Flank and crest, vicinity of 35°N; FF,GG,HH,VV[d])										
22	INMD 50	32°N, 39°W	3500	5	0.60[b]	calcareous	1.0	Box Core	.17	[53]
24	FAMOUS 527-3	36°45.5'N,33°15.3'W	2600	76	0.72-0.75	--	2.9	Alvin Push Core	2.6	[8]
North Atlantic (N of 50°N; SS,TT,UU,WW[d])										
23	KN51 Core 3	52°10.3'N,42°07.8'W	4169	13	0.60[b]	--	--	Gravity Core	.65	This Study
26	KN51 Core 7	52°39.5'N,35°31.6'W	3710	43	0.60[b]	--	--	Gravity Core	2.2	"
27	KN51 Core 20	52°22.8'N,32°17.2'W	2575	27	0.60[b]	--	--	Gravity Core	1.4	"
35	KN51 Core 13	56°16.2'N,24°24.1'W	3200	12	0.60[b]	--	--	Gravity Core	.60	"
36	KN54 BC52	61°55.7'N,17°13.2'W	2195	46	0.55-0.71[b]	--	--	Box Core	2.30	"
37	KN54 BC50	60°07.9'N,16°05.0'W	1885	19	0.62[b]	--	--	Box Core	.95	"
38	KN54 BC40	63°50.0'N,00°54.0'E	2197	30	0.49-0.67	--	--	Box Core	1.5	"
40	Newfoundland slope/rise (>2000m)	~50°N,47°W	1500-3200	11±6(n=3)	.7	terrigenous clay	9	Box Core	.55	[47]
Venezuela Basin (EE[d])										
41	Venezuela Basin	~14°N,~66°W	3500-5050	45±21(n=4) 40±18(n=10)	-	terrigenous/carbonate	--	Box Core	1.0 .89	[46]

[a] Value given is mean ± one standard deviation.

[b] Estimated core bulk density.

[c] Average sedimentation rate stated in reference.

[d] Mean water column ^{210}Pb deficiency from indicated stations (Table 1) used to normalize sediment ^{210}Pb inventories.

and ^{226}Ra activities (dpm/g), using equation (2):

$$I = \sum_i \left(\rho_i A^i_{xs} \Delta X_i \right) \qquad (2)$$

where: I = inventory of excess ^{210}Pb (dpm/cm^2); ρ_i = dry bulk density (g dry sediment/cm^3 wet sediment) of the ith depth interval; A^i_{xs} = excess ^{210}Pb activity (dpm/g) of the ith depth interval, calculated as total $^{A}210_{Pb} - {}^{A}226_{Ra}$; and ΔX_i = thickness of ith depth interval (cm). It is often the case that ^{210}Pb and ^{226}Ra are not measured on every sample and interpolation is required to calculate inventories. Dry bulk densities, when not measured or reported, have been estimated from regional values obtained from nearby sites or from sediment composition parameters such as the percentage of calcium carbonate [30].

One constraint in applying eq. (2) is whether

^{210}Pb measurements are made deep enough in a core so that equilibrium is reached with ^{226}Ra. In general, we have considered this condition satisfied if excess ^{210}Pb decreases to 10% of its interfacial value. In other cases, an inventory can still be calculated by fitting an exponential through the data and integrating. The sites for which sediment ^{210}Pb inventories have been calculated are shown in Figs. 1 and 2 and the data are summarized in Table 2.

3.2. *^{210}Pb scavenging in the North Atlantic*

The Nares and Hatteras Abyssal Plains in the Northwest Atlantic Ocean provide a useful example of the approaches outlined above for determining the extent of ^{210}Pb removal from the water column because water column profiles of ^{210}Pb and ^{226}Ra, fluxes of ^{210}Pb in sediment traps and inventories in bottom sediments have all been measured at these sites.

Water column profiles of ^{210}Pb and ^{226}Ra show ^{210}Pb excesses in surface waters (Fig. 4, Table 3). This pattern is due to the atmospheric supply of ^{210}Pb to the surface ocean, yet calculation of the inventory of "excess" ^{210}Pb relative to ^{226}Ra in the upper 1000 m produces values considerably less than expected from the atmospheric ^{210}Pb flux at these sites. This indicates that most ($\sim$ 80%) of the atmospherically-derived ^{210}Pb has been removed by scavenging. Below about 1000 m, ^{210}Pb activities are deficient relative to ^{226}Ra and this pattern persists to the sea floor. The ^{210}Pb profiles at the two sites are quite similar to each other and to previous measurements in the area by Boyle et al. [31]. This indicates relatively little lateral variability in this region of the open Northwest Atlantic.

Integrating the water column ^{226}Ra activity gives 68 dpm/cm^2 at Nares and 58 dpm/cm^2 at Hatteras (Table 1). The difference is due to the greater water depth at Nares. The atmospheric flux at both sites is taken to be the Bermuda value, 0.69 dpm/cm^2/yr [28], which produces a ^{210}Pb standing crop of 22 dpm/cm^2, and the total supply of ^{210}Pb to the water column is 90 dpm/cm^2 at Nares and 80 dpm/cm^2 at Hatteras. The ^{210}Pb present in the water column, obtained by integrating the ^{210}Pb profiles (Fig. 4), is 51 dpm/cm^2 at Nares and 43 dpm/cm^2 at Hatteras. Thus 39 and 37 dpm ^{210}Pb/cm^2 or about 45% of the total supply of ^{210}Pb has been scavenged at Nares and Hatteras, respectively.

TABLE 3

^{210}Pb in water samples from the Nares and Hatteras Abyssal Plains, Northwest Atlantic

Depth (m)	^{210}Pb (dpm/100 kg)
Nares Abyssal Plain (23°12.0′N, 63°58.9′W, 5840 m)	
3	19.0±1.0
834	12.2±1.0
1060	7.9±1.0
1442	7.1±0.7
2550	9.2±2.2
3331	7.5±0.7
4124	6.4±0.6
4994	6.1±0.6
5681	7.6±0.6
5788	6.8±0.5
Hatteras Abyssal Plain (32°48.6′N, 70°44.6′W, 5400 m)	
3	14.7±1.7
158	12.3±1.6
208	11.7±1.4
857	8.8±0.9
978	7.2±0.7
1592	9.5±0.8
2945	8.7±0.8
3384	7.2±0.7
3978	3.5±0.6
4584	5.8±0.6
5300	6.1±0.7

These values can be compared with measurements of the vertical flux of ^{210}Pb at the Nares site. Sediment trap samples were collected over successive intervals of 78 days for a one year period (1983–1984) at two depths, 1464 and 4832 m. Samples taken at both depths show good correlation between both mass flux and organic carbon flux and ^{210}Pb flux (Fig. 5). A similar observation has been made by Moore and Dymond [33] for sediment trap samples collected in the Pacific. These correlations can be explained in the context of the scavenging model for reactive nuclides proposed by Bacon and Anderson [34]. In this model, radionuclides such as ^{210}Pb are adsorbed onto small suspended particles which sink only very slowly. The small particles and associated radionuclides can be packaged into larger, rapidly sinking particles such as fecal pellets which are removed from the water column. The latter constitute most of the mass flux recorded in sediment traps. Thus an increase in bulk flux or flux of

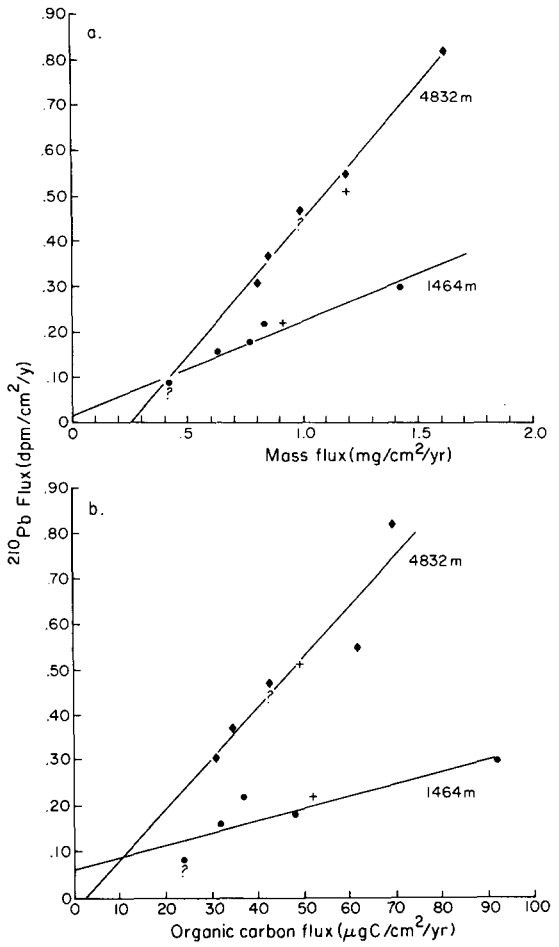

Fig. 5. ^{210}Pb flux (dpm/cm^2/yr) vs a) mass flux (mg/cm^2/yr) and b) organic carbon flux (μg/cm^2/yr) for sediment traps deployed at 1464 and 4832 in the Nares Abyssal Plain. The samples at each depth were collected sequentially by means of a rotating cup. Each point corresponds to ~ 78 days of sample collection. Points marked with question marks denote the final cup which was open at retrieval and may have lost material. These values were not used in computing mean fluxes at each depth, denoted by the crosses. Lines through the data are linear least square fits.

large particles results in an increased flux of packaged small particles and associated ^{210}Pb (Fig. 5).

The second observation we make regarding the sediment trap data is that the mean flux of ^{210}Pb increases from 0.22 to 0.51 dpm/cm^2/yr between the 1464 and 4832 m traps (Fig. 5). This is a result of continued uptake of ^{210}Pb on small particles as they are transferred through the water column by packaging into large particles and the disintegration of the large particles back into small particles. Because production of ^{210}Pb from ^{226}Ra decay occurs throughout the water column, additional scavenging can take place as the particles sink. The mean flux of ^{210}Pb recorded in the 4832 m trap supports a steady-state removal of 16 dpm ^{210}Pb/cm^2 from the water column and should be comparable to the inventory recorded in sediments at the site. We note that the flux of ^{210}Pb measured in the sediment trap accounts for less than half of the ^{210}Pb removal from the water column (39 dpm/cm^2).

Sediment profiles of ^{210}Pb from cores taken at Nares show excess ^{210}Pb present to depths of 3–8 cm (Appendix), and inventories calculated from these profiles vary from 3.6 to 14.0 dpm/cm^2. This variation occurs not only on the scale of sampling at the Nares Abyssal Plain (10–50 km between stations), but also on the scale of a single box core. For example, Smith et al. [14] measured excess ^{210}Pb on subcores of box cores taken in the northeast Atlantic and showed that inventories varied by as much as a factor of 6 for two subcores taken within ~ 25 cm of one another. This pattern is probably due to patchiness in the density and activity of the benthic fauna, which serves to distribute ^{210}Pb throughout the upper decimeter of deep-sea sediments. It is likely that integrating over a larger area of the sea floor when taking samples for inventories of ^{210}Pb or other short-lived radionuclides will reduce the variability in the measured inventories. Indeed, Cochran and Krishnaswami [36] sampled the entire area of these 2500 cm^2 box cores taken in the North Equatorial Pacific and found relatively little variation in $^{210}Pb_{xs}$ inventory (35–40 dpm/cm^2). However, in areas where the bottom is disturbed physically on a frequent basis, such as the HEBBLE site in the Northwest Atlantic [37], inventories of $^{210}Pb_{xs}$ may be quite variable even when large areas of the sea floor are sampled [38]. In general most of the data summarized in Table 2 are based on small area subcores of box cores, and mean values of $^{210}Pb_{xs}$ inventory for a given area have large standard deviations.

At Hatteras and Nares, mean sediment $^{210}Pb_{xs}$ inventories are 20 ± 6 and 9 ± 4 dpm/cm^2 (Table 2). These values bracket the inventory expected from the ^{210}Pb flux in the deep sediment trap at Nares (16 dpm/cm^2), but both sediment trap and

bottom sediments record lower fluxes than those required to support the ^{210}Pb deficiency in the overlying water column (~ 38 dpm/cm^2). The similarity in sediment trap and bottom sediment ^{210}Pb fluxes suggests that scavenging of ^{210}Pb at the sediment–water interface is not large at these sites. Indeed, Spencer et al. [4] calculated it to be $< 4\%$ of the total removal of ^{210}Pb for the North Atlantic as a whole. Thus about 50% of the ^{210}Pb scavenged from the water column at the Nares and Hatteras Abyssal Plains is not carried to the bottom locally but is transported out of the area to sinks elsewhere.

In order to compare sediment inventories in different parts of the Atlantic, we normalize them to the deficiency of ^{210}Pb in the overlying water column (Fig. 6a). Low values ($\ll 100\%$) of the normalized inventory, as observed at Nares or Hatteras, indicate that the sink for most of the scavenged ^{210}Pb is not local. Values close to 100% indicate that all of the ^{210}Pb removed from the water column is present in the sediments below, and values greater than 100% imply import of ^{210}Pb to the area. Although there is considerable scatter due to the small scale spatial variability of ^{210}Pb distributions in the sediments, the pattern of normalized sediment ^{210}Pb inventories in the North Atlantic is one of generally low values (frequently $\leq 50\%$) south of about 45° N and high values north of 50° N ($> 50\%$). Exceptions to the pattern south of 45° N include a core taken in a sediment pond on the Mid-Atlantic Ridge and cores taken at the HEBBLE site [38].

Several factors might cause the trend toward greater normalized sediment ^{210}Pb inventories in the high latitudes. The normalized sediment inventories must in part reflect the vertical flux of particles at these open ocean sites, and an important component of the particulate flux is the flux of biogenic particles. This flux is linked to the primary production of an area and especially to the new production [39–42]. Indeed, Fisher et al. [32] have shown that it is possible to accurately estimate the flux of particle reactive radionuclides at open ocean sites from knowledge of dissolved radionuclide concentrations, concentration factors on biogenic particles and new production. A correlation between organic carbon flux and ^{210}Pb flux has been demonstrated by Moore and Dymond [33] for sediment trap samples from the Pacific and for our North Atlantic samples (Fig. 5b), and Moore and Dymond [33] suggested that a similar relationship might be expected between the biogenic flux and sediment inventories of excess ^{210}Pb. Estimates of new production in oligotrophic central gyre areas (e.g. mid-latitude northwest Atlantic) are lower by a factor of two compared to the transitional waters between subtropical and subpolar zones (e.g. high-latitude North Atlantic) [40]. Satellite photographs also show that the equatorial Pacific and high-latitude North Atlantic have higher productivities than central gyre areas such as the central northwest or northeast Atlantic [43]. Thus the data suggest that the greater the flux of biogenic particles in an area, the greater the supply of ^{210}Pb to the bottom and the higher the normalized sediment ^{210}Pb inventories.

In order to construct a proper ^{210}Pb balance for the North Atlantic, sample coverage for sediment and water column data must be sufficient to permit calculation of weighted areal averages. At present the data are insufficient to make such calculations, but the high-latitude North Atlantic does appear to represent a large enough region to balance the ^{210}Pb-deficient sediments of the central gyre. Transport of ^{210}Pb from areas of weak removal to strong sinks has been documented, particularly in the case of ocean margins where upwelling is occurring [6]. Indeed, Bacon et al. [3] and Cochran et al. [5] have calculated that transport of ^{210}Pb by eddy diffusion from the open ocean to strong sinks was effective for distances of about 2000 km.

Oceanic margins can serve as strong sinks for reactive radionuclides, but the western margin of the North Atlantic, represented by the continental shelf and coastal areas off the northeastern USA, does not represent an important sink for ^{210}Pb imported from elsewhere [44,45]. Instead ^{210}Pb in sediments of this area appears to be in balance with local supply. The eastern margin of the North Atlantic may represent an important sink for ^{210}Pb as does the analogous area of the eastern Pacific off California and the Washington shelf [6,7], but at present data are lacking to assess the importance of this area.

Several other areas have surplus inventories of ^{210}Pb$_{xs}$ in their sediments (Fig. 6a). For example, sediments of the HEBBLE site have been shown to have consistently high, though variable, invento-

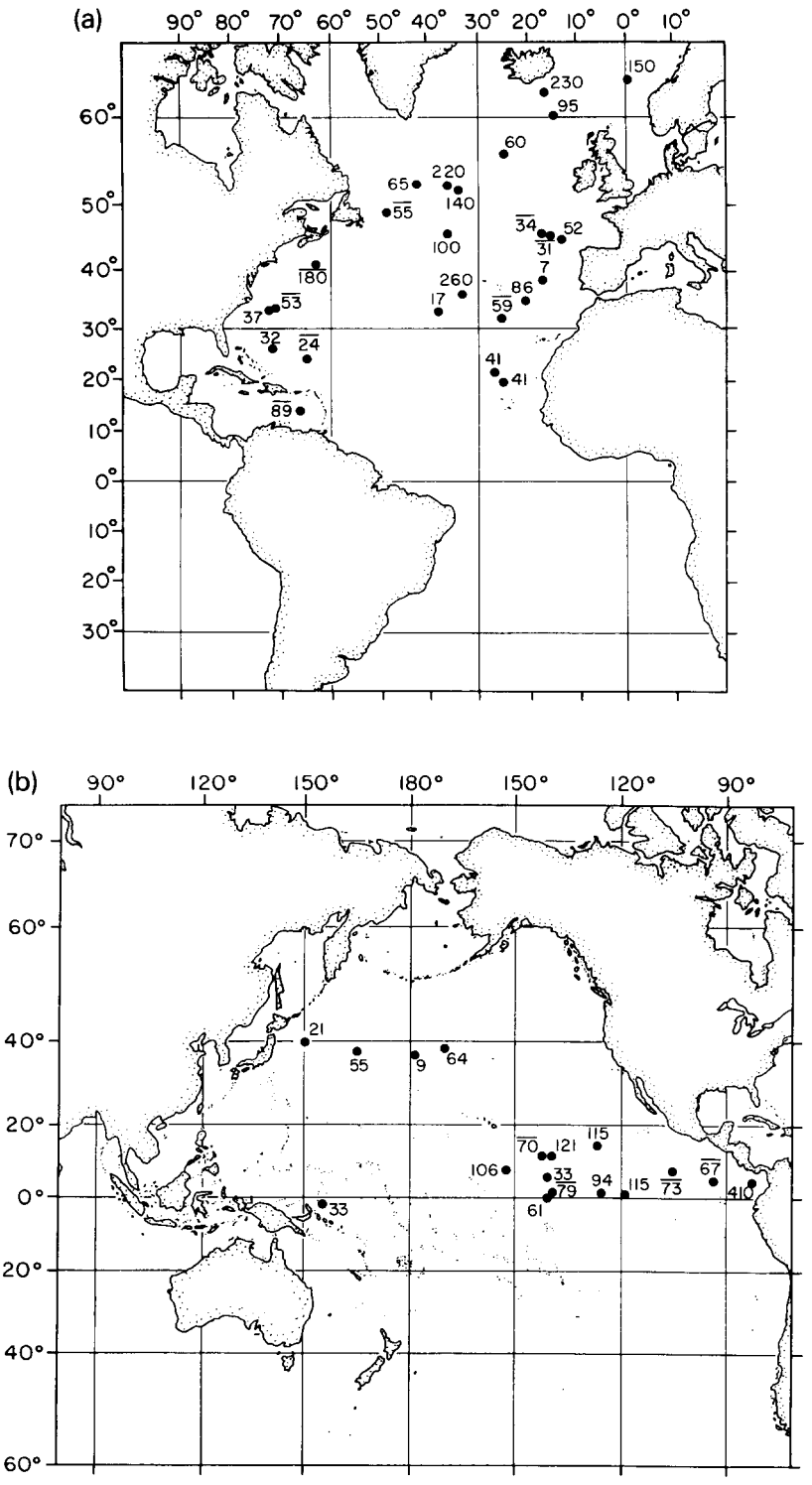

Fig. 6. Inventories of excess ^{210}Pb in deep-sea sediments. The values have been normalized to the ^{210}Pb scavenged from the overlying water column (as calculated from the water column data) and are expressed as percent. A value of 100 implies that all ^{210}Pb scavenged from the overlying water column is present in the bottom sediments. Solid bar over value indicates average of several cores at a given site (Table 2). See text for discussion. (a) North Atlantic; (b) North Pacific.

ries of excess ^{210}Pb [13,38]. This area is characterized by frequent and intense benthic "storms" which produce very high concentrations of suspended sediment. High ^{210}Pb inventories also are present in sediments of the Venezuela Basin [46], although the highest inventories in this area may be due to turbidity flows rather than enhanced in situ scavenging of ^{210}Pb. Continental slope sediments off Newfoundland also are characterized by high ^{210}Pb inventories [47]. Deeper sites on the slope and rise have lower inventories of ^{210}Pb, possibly due to the presence of the Western Boundary Undercurrent. Although these areas offset the ^{210}Pb-deficient sediments of the central gyre, they do not seem extensive enough to balance the deficit, especially in comparison with the high-latitude sediments.

3.3. *^{210}Pb scavenging in the North Pacific*

The North Pacific shows several interesting differences in ^{210}Pb scavenging relative to the North Atlantic. In general, ^{210}Pb is scavenged less effectively in the North Pacific. Only about 20% of the ^{210}Pb available for scavenging is removed from the water column and, as a consequence, the residence time of ^{210}Pb with respect to scavenging is longer in the Pacific than the Atlantic (on average 140 $\pm$ 60 yr in the Pacific vs. 35 $\pm$ 15 yr in the Atlantic; Table 1, Fig. 3).

In part, this difference is created by considering the ocean as a single box in which scavenging of ^{210}Pb from the surface and deep ocean are considered together. Scavenging in the surface ocean is more rapid than in the deep ocean, and the introduction of ^{210}Pb into the surface ocean is principally by the atmospheric flux. Thus a water column in which the atmospheric flux is a larger fraction of the total ^{210}Pb supply (from the atmosphere and from in situ ^{226}Ra decay) will have a shorter scavenging residence time for ^{210}Pb in a single box model, if all other factors are comparable. Indeed, the atmospheric flux of ^{210}Pb is larger in the North Atlantic than North Pacific [27,29]. However, if we assume that essentially all of the atmospheric ^{210}Pb flux is scavenged (see section 3.2), we can correct the observed ^{210}Pb deficiency in the water column to obtain that due to scavenging of ^{210}Pb produced in situ by ^{226}Ra. Production of ^{210}Pb from ^{226}Ra is dominated by ^{226}Ra decay in the deep ocean and thus the corrected ^{210}Pb deficiency represents scavenging from the deep ocean. When this correction is made, the difference in scavenging residence time in the two oceans remains but is less pronounced (200 $\pm$ 100 yr for the Pacific vs. 80 $\pm$ 30 yr for the Atlantic).

Other possibilities which explain the difference in scavenging effectiveness include differences in particle fluxes and proximity to strong sinks. Although the primary productivity and new production of the equatorial Pacific are relatively high, the deeper, more acidic water column is less favorable for the preservation of sinking calcium carbonate tests. Dissolution of sinking tests and release of associated radionuclides could lower the scavenging effectiveness of the Pacific.

The high inventories of excess ^{210}Pb in eastern Pacific margin sediments [6], including those of the Panama Basin [51, Table 2], indicate that such areas are important sinks for reactive radionuclides. The effect of such sinks on ^{210}Pb removal from the water column at an open ocean site depends on the rate of transport of ^{210}Pb to the sink and the half-life of ^{210}Pb [3,5]. If the transport of ^{210}Pb to margin sinks is comparable in the Atlantic and Pacific, the considerably larger size of the Pacific suggests that more of this ocean is relatively unaffected by distant sinks. This hypothesis predicts that scavenging of ^{210}Pb from open Pacific sites such as those of the equatorial region should be dominated by vertical transport and that sediment inventories of $^{210}Pb_{xs}$ at these sites should equal the ^{210}Pb scavenged from the overlying water column. Indeed, Fig. 6b shows this to be the case. The mean $^{210}Pb_{xs}$ inventory in cores from the open North Equatorial Pacific is 26 $\pm$ 13 dpm/cm^2 (mean $\pm$ 1σ of all cores, Table 2) and this compares favorably with the mean water column ^{210}Pb deficiency of 33 $\pm$ 11 dpm/cm^2. Thus it appears that the sediments of the North Equatorial Pacific are in balance with ^{210}Pb scavenged from the overlying water column, and that scavenging of ^{210}Pb in this area is dominated by processes operating in a vertical sense. The North Atlantic, by contrast, shows strong isopycnal transport of ^{210}Pb out of the oligotrophic, mid-latitudes to stronger sinks in the high latitudes or possibly the eastern margin.

Elsewhere in the Pacific, lateral transport to sinks may be important. It is interesting to note that the four mid-latitude Pacific cores for which

^{210}Pb inventories are available (Fig. 2, [52]) show lower normalized inventories, on the average, than do the equatorial cores. A gradient in productivity also exists in the North Pacific, with relatively high values in the equatorial and high latitudes. It is possible that a pattern of normalized sediment inventories similar to the North Atlantic exists in the North Pacific, with low values in the mid-latitudes and high values in the high latitudes (and equatorial region). Additional sediment data from the high latitude Pacific will enable this hypothesis to be tested.

5. Conclusions

A ^{210}Pb balance for the open ocean can be constructed by comparing the deficiency of ^{210}Pb in a given water column (relative to its supply from the atmosphere and in situ decay of ^{226}Ra) with inventories of excess ^{210}Pb in underlying sediments. The "scavenging effectiveness" of ^{210}Pb from the entire water column, defined as the ratio of ^{210}Pb water column deficiency to total supply, is about 20% in the North Equatorial Pacific and about 50% in the North Atlantic. These values reflect both removal of ^{210}Pb onto sinking particles and lateral transport of ^{210}Pb to strong sinks, and the differences remain even when corrections are made for difference in scavenging rate and ^{210}Pb supply in the surface relative to the deep ocean.

A measure of the relative importance of vertical and lateral processes in ^{210}Pb scavenging is derived from the ratio of excess ^{210}Pb inventories in deep-sea sediments to the deficiency of ^{210}Pb in the overlying water column. In the North Equatorial Pacific, virtually all ($\geq 80\%$) of the ^{210}Pb scavenged from the water column is present in the underlying sediments. This suggests that ^{210}Pb supplied locally to the surface waters and produced from decay of ^{226}Ra in the overlying water column is scavenged onto sinking particles and transported to the bottom.

In contrast, sediments of the mid-latitude North Atlantic account for only $\sim 40\%$ of the ^{210}Pb scavenged from the overlying water column, and the remainder apparently is transported to sinks outside the area. The data coverage is insufficient to permit a quantitative mass balance to be constructed, but cores taken in areas of frequent bottom disturbances, such as the HEBBLE site, and underlying the relatively high-productivity waters of the high latitudes have surpluses of excess ^{210}Pb. The latter may be of sufficient areal extent to balance the deficits observed in sediments of the oligotrophic central North Atlantic.

Acknowledgements

The data presented in this paper were generated from funding from several sources. We are particularly grateful to the National Science Foundation for supporting the work in the North Equatorial Pacific (Grants OCE 8215747 and 8400072 to JKC) and North Atlantic (Grant OCE 8819544 to JKC and OCE-8614545 to HDL). The work at the Nares and Hatteras Abyssal Plains was supported by Sandia National Laboratories as part of its Subseabed and Low Level Radioactive Waste Disposal Programs. Discussions with our colleagues, particularly K. Turekian, N. Fisher, R. Aller and M. Scranton have helped clarify several of the ideas presented here, and reviewer's comments from M. Bacon and W. Moore and an anonymous reviewer are appreciated. Mary Ann Lau expertly typed several drafts of the manuscript. An earlier version of this paper was presented at the International Congress of Geochemistry and Cosmochemistry held in Paris in September, 1988, and travel support from the meeting organizers to JKC is gratefully acknowledged. This is Contribution No. 692 from the Marine Sciences Research Center and No. 7234 from Woods Hole Oceanographic Institution.

APPENDIX

^{210}Pb and ^{226}Ra measurements for deep-sea sediment cores from the Atlantic and Pacific Oceans

Depth (cm)	Bulk density (g_{dry}/cm^3_{wet})	^{210}Pb [a]	^{226}Ra [a]	^{210}Pb [b] (dpm/g)	^{226}Ra [c]	$^{210}Pb_{xs}$ [d]
Nares Abyssal Plain						
BC 02 (22°42.7′N, 64°20.2′W, 5775 m)						
0–1	0.78 [e]	13.8±0.8	–	13.4±0.7	2.7±0.1	10.9±0.7
1–2		3.9±0.7	–	4.4±0.3	3.1±0.1	1.1±0.4
2–3		3.9±0.7	–	3.2±0.2	3.1±0.1	0.5±0.5
4–5		4.7±0.4	–	4.9±0.3	3.3±0.1	1.5±0.3
6–7		4.3±0.7	–	3.2±0.2	3.6±0.1	0.2±0.8
10–12		5.2±0.4	–	4.5±0.2	4.4±0.1	0.5±0.5
18–20		4.6±0.5	–	4.2±0.3	4.9±0.1	−0.4±0.3
$\Sigma^{210}Pb_{xs}$ (dpm/cm^2)						12
BC 08 (23°32.8′N, 64°30.2′W, 5775 m)						
0–1	0.78	16.2±0.8	–	15.8±0.7	2.9±0.1	12.9±0.7
1–2		5.5±0.6	–	5.4±0.2	3.3±0.1	2.1±0.2
2–3		4.3±0.6	–	3.9±0.3	3.3±0.1	0.6±0.3 [g]
4–5		5.1±0.7	–	–	–	0.0±0.4 [g]
8–9		6.0±0.8	–	–	–	0.9±1.4 [g]
14–16		5.2±0.5	–	–	–	0.1±1.4 [g]
$\Sigma^{210}Pb_{xs}$ (dpm/cm^2)						12
BC 09 (23°12.0′N, 64°45.4′W, 5775 m)						
0–1	0.78	7.7±0.7	–	7.5±0.3	3.9±0.1	3.6±0.3
1–2		5.4±0.7	–	5.0±0.2	3.5±0.1	1.5±0.2
2–3		4.7±0.8	–	5.5±0.3	3.4±0.1	2.1±0.3
6–7		3.9±0.5	–	–	–	−1.2±1.3 [g]
10–12		4.5±0.5	–	–	–	−0.6±1.3 [g]
18–20		5.3±0.4	–	–	–	0.2±1.3 [g]
$\Sigma^{210}Pb_{xs}$ (dpm/cm^2)						8
BC 15 (23°16.7′N, 63°53.6′W, 5779 m)						
0–1	0.78	5.6±1.5	–	6.1±0.2	3.2±0.1	2.9±0.2
1–2		4.4±0.7	–	4.4±0.1	3.9±0.1	0.5±0.1
2–3		5.6±0.8	–	4.3±0.3	3.5±0.1	0.8±0.3
4–5		4.0±0.7	–	–	–	−1.1±1.4 [g]
8–9		7.1±0.8	–	–	–	2.0±1.4 [g]
14–16		5.3±0.5	–	–	–	0.2±1.3 [g]
$\Sigma^{210}Pb_{xs}$ (dpm/cm^2)						4
BC 18 (22°41.5′N, 63°27.3′W, 5768 m)						
0–1	0.78	5.3±0.7	–	5.0±0.2	3.7±0.1	1.3±0.2
1–2		5.6±0.7	–	5.0±0.1	4.0±0.1	1.0±0.1
2–3		5.7±0.8	–	4.6±0.3	4.0±0.1	0.6±0.3
6–7		5.6±0.7	–	–	–	0.5±1.4 [g]
10–12		5.2±0.7	–	–	–	0.1±1.4 [g]
18–20		3.0±0.7	–	–	–	−2.1±1.4 [g]
20–24		2.0±0.7	–	–	–	−3.1±1.4 [g]
$\Sigma^{210}Pb_{xs}$ (dpm/cm^2)						4
BC 23 (23°01.4′N, 64°13.6′W, 5777 m)						
0–1	0.78	12.6±0.9	–	11.5±0.4	2.7±0.1	8.8±0.4
1–2		4.6±0.6	–	4.9±0.3	3.1±0.1	1.8±0.3
2–3		3.7±0.7	–	3.8±0.3	3.3±0.1	0.5±0.3 [g]
4–5		5.7±0.7	–	–	–	0.6±1.4 [g]
8–9		5.1±0.5	–	–	–	0.0±1.3 [g]
14–16		5.3±0.5	–	–	–	0.2±1.3 [g]
$\Sigma^{210}Pb_{xs}$ (dpm/cm^2)						10

APPENDIX (continued)

Depth (cm)	Bulk density (g_{dry}/cm^3_{wet})	^{210}Pb [a]	^{226}Ra [a]	^{210}Pb [b] (dpm/g)	^{226}Ra [c]	$^{210}Pb_{xs}$ [d]
BC 25 (22°57.7′N, 64°10.5′W, 5775 m)						
0–1	0.78	8.1±0.5	–	8.5±0.4	3.0±0.1	5.5±0.4
1–2		5.2±0.3	–	4.7±0.2	3.0±0.1	1.7±0.2
2–3		5.0±0.5	–	4.6±0.3	3.5±0.1	1.1±0.3 [g]
6–7		5.4±0.7	–	–	–	0.3±1.4 [g]
10–12		6.4±0.5	–	–	–	1.3±1.3 [g]
18–20		5.4±0.5	–	–	–	0.3±1.3 [g]
$\Sigma^{210}Pb_{xs}$ (dpm/cm^2)						8
BC 32 (22°13.9′N, 63°15.5′W, 5719 m)						
0–1	0.78	12.9±0.7	–	11.4±0.8	3.2±0.3	9.0±1.1
1–2		7.6±0.8	–	6.6±0.7	3.7±0.4	3.4±0.8
2–3		7.3±0.7	–	7.3±0.7	4.4±0.4	2.9±0.8
4–5		5.7±0.6	–	5.6±0.8	4.9±0.5	0.8±0.9
6–7		5.6±0.8	–	5.9±0.9	5.8±0.6	0.0±1.1
10–12		6.9±0.8	–	–	6.6±0.7	0.3±1.1
18–20		7.1±0.8	–	–	6.6±0.7	0.5±1.1
28–32		6.9±0.8	–	–	5.6±0.6	1.3±1.0
$\Sigma^{210}Pb_{xs}$ (dpm/cm^2)						14
North Atlantic						
KN54 BC52 (61°55.7′N, 17°13.2′W, 2195 m)						
0–1	0.6	20.5±0.8	2.1±0.2	–	–	26.1±1.5
1–2	0.6	10.6±0.6	1.9±0.2	–	–	12.4±1.2
2–3	0.7	9.7±0.6	2.2±0.2	–	–	10.6±1.2
3–4	0.6	6.5±0.5	1.7±0.2	–	–	6.8±1.0
4–6	0.6	5.5±0.6	2.4±0.2	–	–	4.4±1.2
6–8	0.6	5.0±0.7	2.6±0.2	–	–	3.4±1.3
8–10	0.6	3.2±0.5	2.7±0.2	–	–	0.7±1.0
10–12	0.6	3.2±0.6	2.9±0.2	–	–	0.4±1.2
$\Sigma^{210}Pb_{xs}$ (dpm/cm^2)						46
KN54 BC50 (60°07.9′N, 16°05.0′W, 1885 m)						
0–1	0.6 [f]	10.7±0.9	4.4±0.3	–	–	10.2±1.8
1–2		7.1±0.7	4.5±0.2	–	–	4.1±1.5
2–3		7.0±1.1	4.7±0.4	–	–	3.8±2.3
3–4		6.5±0.8	4.0±0.3	–	–	4.0±1.8
4–6		6.6±0.8	4.3±0.3	–	–	3.7±1.8
6–8		4.7±0.7	3.2±0.2	–	–	2.4±1.6
8–10		3.9±0.7	3.1±0.2	–	–	1.2±1.6
10–12		3.4±0.7	3.1±0.2	–	–	0.5±1.5
$\Sigma^{210}Pb_{xs}$ (dpm/cm^2)						23
KN54 BC40 (63°50.0′N, 00°54.0′W, 2197 m)						
0–1	0.5	–	–	–	–	–
1–2	0.5	13.3±0.7	2.0±0.2	–	–	16.0±1.3
2–3	0.5	–	–	–	–	–
3–4	0.5	7.3±0.8	2.7±0.3	–	–	6.6±1.6
4–5	0.6	–	–	–	–	–
5–6	0.7	4.1±0.9	3.7±0.4	–	–	0.6±1.8
$\Sigma^{210}Pb_{xs}$ (dpm/cm^2)						31
KN54 Core 15 (45°36.5′N, 12°34.3′W, 4900 m)						
0–1	0.6 [e]	5.7±0.9	1.8±0.3	–	–	5.2±1.5
1–2		5.2±0.9	2.1±0.3	–	–	4.0±1.5
2–3		5.3±0.9	4.0±0.4	–	–	1.7±1.8
3–4		3.3±0.9	2.0±0.2	–	–	1.7±1.5

APPENDIX (continued)

Depth (cm)	Bulk density (g_{dry}/cm^3_{wet})	^{210}Pb [a]	^{226}Ra [a]	^{210}Pb [b] (dpm/g)	^{226}Ra [c]	$^{210}Pb_{xs}$ [d]
KN54 Core 15 (45°36.5'N, 12°34.3'W, 4900 m)						
4–5		6.5±0.9	3.2±0.3	–	–	4.5±1.5
5–6		3.7±0.7	2.3±0.2	–	–	1.8±1.1
6–7		4.2±0.8	2.8±0.2	–	–	1.9±1.3
7–8		4.0±0.8	2.8±0.2	–	–	1.5±1.3
8–9		3.8±0.8	3.2±0.2	–	–	0.9±1.3
9–10		3.8±0.6	2.8±0.2	–	–	1.3±1.1
10–12		2.9±0.6	2.8±0.2	–	–	0.0±1.1
$\Sigma^{210}Pb_{xs}$ (dpm/cm^2)						15
KN51 Core 11 (45°14.0'N, 36°04.0'W, 4189 m)						
0–1	0.6 [e]	9.3±1.1	2.4±0.3	–	–	10.2±2.0
1–2		7.7±1.1	2.3±0.3	–	–	8.0±2.0
2–3		3.9±0.8	1.9±0.2	–	–	3.0±1.4
3–4		4.4±0.6	2.0±0.2	–	–	3.5±1.4
4–6		5.5±0.6	2.4±0.2	–	–	4.6±1.1
6–8		5.4±0.6	2.5±0.2	–	–	4.3±1.2
8–10		3.8±0.6	2.6±0.2	–	–	1.8±1.1
10–12		3.4±0.7	3.2±0.2	–	–	0.3±1.3
12–14		3.3±0.6	2.3±0.2	–	–	1.5±1.1
$\Sigma^{210}Pb_{xs}$ (dpm/cm^2)						30
KN51 Core 7 (52°39.5'N, 35°31.6'W, 3710 m)						
0–1	0.6 [e]	16.5±0.9	1.8±0.3	–	–	21.6±1.8
1–2		11.1±1.6	3.3±0.5	–	–	11.4±3.1
2–3		6.0±1.1	3.0±0.4	–	–	4.4±2.3
3–4		5.1±0.5	3.0±0.2	–	–	3.2±1.1
4–6		6.4±0.5	2.4±0.2	–	–	5.8±1.0
6–8		6.7±0.8	3.1±0.3	–	–	5.4±1.5
8–10		4.8±0.6	2.1±0.2	–	–	4.0±1.2
10–12		4.6±0.8	2.1±0.2	–	–	3.7±1.4
$\Sigma^{210}Pb_{xs}$ (dpm/cm^2)						47
KN51 Core 20 (52°22.8'N, 32°17.2'W, 2575 m)						
0–1	0.6 [e]	17.0±1.9	2.7±0.5	–	–	21.1±3.6
1–3		7.1±1.0	3.0±0.3	–	–	6.1±1.8
3–4		8.0±1.2	3.7±0.4	–	–	6.4±2.3
4–5		4.4±0.8	3.0±0.3	–	–	2.0±1.6
5–6		4.4±0.9	3.1±0.4	–	–	1.9±1.9
6–7		5.0±0.7	3.6±0.3	–	–	2.1±1.4
7–8		3.4±0.8	2.3±0.3	–	–	1.7±1.5
8–9		2.7±0.8	2.6±0.3	–	–	0.0±1.5
9–10		3.0±0.8	2.6±0.2	–	–	0.5±1.5
10–11		2.6±0.8	2.6±0.2	–	–	0.0±1.4
$\Sigma^{210}Pb_{xs}$ (dpm/cm^2)						29
KN51 Core 13 (56°16.2'N, 24°24.1'W, 3200 m)						
0–1	0.6 [e]	4.3±0.5	1.0±0.2	–	–	4.7±1.0
1–2		4.7±1.2	2.0±0.4	–	–	4.0±2.3
2–3		4.1±0.9	1.1±0.2	–	–	4.4±1.6
3–4		2.8±0.5	0.9±0.2	–	–	2.6±0.9
4–5		2.3±0.5	1.6±0.2	–	–	1.0±1.0
5–6		2.2±0.5	1.5±0.2	–	–	1.0±1.0
6–7		2.4±0.6	1.5±0.2	–	–	1.4±1.1
7–8		1.8±0.7	1.2±0.2	–	–	0.9±1.3
8–9		1.7±0.6	1.7±0.2	–	–	0.3±1.1
9–10		2.3±0.5	2.3±0.2	–	–	0.0±1.0
10–12		1.4±0.6	1.3±0.2	–	–	0.2±1.2
$\Sigma^{210}Pb_{xs}$ (dpm/cm^2)						12

APPENDIX (continued)

Depth (cm)	Bulk density (g_{dry}/cm^3_{wet})	^{210}Pb [a]	^{226}Ra [a]	^{210}Pb [b] (dpm/g)	^{226}Ra [c]	$^{210}Pb_{xs}$ [d]
KN51 Core 3 (52°10.3′N, 42′07.8′W, 4169 m)						
0–1	0.6 [e]	6.2±0.8	1.7±0.2	–	–	6.7±1.5
1–2		3.9±0.8	1.6±0.2	–	–	3.5±1.4
2–3		3.1±0.9	2.4±0.4	–	–	0.6±2.0
3–4		3.5±0.7	1.6±0.2	–	–	2.8±1.4
4–6		3.4±0.6	1.8±0.2	–	–	2.3±1.1
6–8		3.3±0.6	2.0±0.2	–	–	2.0±1.2
8–10		2.5±0.6	2.1±0.2	–	–	0.6±1.2
10–12		1.8±0.6	1.7±0.2	–	–	0.1±1.1
$\Sigma^{210}Pb_{xs}$ (dpm/cm^2)						14
North Equatorial Pacific						
SBC-11 (MANOP Site C: 1°4.6′N, 138°56.1′W, 4470 m)						
Subcore A						
0.0–0.5	0.41	–	–	41.7±1.6	14.2	27.8±2.1
			–	37.3±1.2	12.1	25.5±1.7
0.5–1.0	0.41	–	–	21.2±1.0	13.6	7.8±1.8
1.0–1.5	0.41	–	–	19.7±0.9	13.6	6.1±1.7
1.5–2.0	0.46	–	–	17.4±0.6	13.4	4.1±1.5
2.0–3.0	0.46	–	–	21.7±0.9	14.9	6.9±1.8
3.0–4.0	0.48	–	–	18.9±0.8	14.2	4.7±1.6
4.0–5.0	0.51	–	–	17.2±0.9	14.8	2.5±1.8
5.0–6.0	0.51	–	–	13.6±0.9	–	–
			–	15.4±1.2	13.2	2.5±1.8
6.0–7.0	0.54	–	–	15.0±1.1	13.8	1.4±2.1
7.0–8.0	0.54	–	–	19.2±0.7	12.1	7.3±1.4
8.0–9.0	0.57	–	–	17.4±0.6	12.9	4.7±1.5
9.0–10.0	0.57	–	–	15.2±0.6	12.5	2.8±1.5
10.0–11.0	0.60	–	–	15.1±1.0	11.7	3.9±1.8
11.0–12.0	0.60	–	–	13.3±0.8	–	–
12.0–13.0	0.63	–	–	14.3±1.2	14.1	0.2±2.1
13.0–14.0	0.63	–	–	13.2±0.8	10.4	3.2±1.5
18.0–20.0	0.68	–	–	17.3±1.4	18.4	−1.1±2.6
$\Sigma^{210}Pb_{xs}$ (dpm/cm^2)						30
Subcore B						
0.0–0.5	0.41	–	–	40.1±2.6	13.1	27.6±3.0
0.5–1.0	0.41	–	–	25.2±0.9	13.5	11.9±1.7
1.0–1.5	0.41	–	–	21.5±1.0	14.2	7.3±1.8
1.5–2.0	0.46	–	–	20.9±0.9	13.4	7.7±1.6
3.0–4.0	0.48	–	–	22.3±2.0	14.2	8.1±2.5
4.0–5.0	0.51	–	–	17.3±0.7	–	3.5±1.6 [g]
5.0–6.0	0.51	–	–	17.3±1.2	14.8	2.6±2.0
7.0–8.0	0.54	–	–	27.1±1.4	–	13.6±2.0 [g]
$\Sigma^{210}Pb_{xs}$ (dpm/cm^2)						26
Lander Deployment 1 – Chamber 3 (L1-3)						
L1-3 (MANOP Site C: 1°3.3′N, 138°56.5′W, 4450 m)						
0.0–0.5	0.41	–	–	37.4±0.8	13.5	24.7±1.7
0.5–1.0	0.41	–	–	27.3±0.6	12.9	14.9±1.5
1.0–1.5	0.41	–	–	27.1±0.5	14.4	13.1±1.5
1.5–2.0	0.46	–	–	28.6±0.6	14.9	14.1±1.7
2.0–3.0	0.46	–	–	22.6±0.7	15.0	7.8±1.7
3.0–4.0	0.48	–	–	20.7±0.9	15.0	5.9±1.8
4.0–5.0	0.51	–	–	18.0±0.8	–	3.6±1.8 [c]
5.0–6.0	0.51	–	–	17.6±0.4	13.6	4.1±1.5
7.0–8.0	0.57	–	–	11.6±0.6	16.7	−5.1±1.9
$\Sigma^{210}Pb_{xs}$ (dpm/cm^2)						26.6

APPENDIX (continued)

Depth (cm)	Bulk density (g_{dry}/cm^3_{wet})	^{210}Pb [a]	^{226}Ra [a]	^{210}Pb [b] (dpm/g)	^{226}Ra [c]	$^{210}Pb_{xs}$ [d]
L2-3 (MANOP Site C: 1°3.3'N, 138°56.5'W, 4451 m)						
0.0–0.5	0.41	–	–	41.7 ± 1.6	14.2	27.8 ± 2.1
0.0–0.5	0.41	–	–	35.9 ± 0.8	12.3	24.3 ± 1.5
0.5–1.0	0.41	–	–	28.7 ± 0.6	13.3	15.9 ± 1.5
1.0–1.5	0.41	–	–	26.3 ± 0.9	12.1	14.6 ± 1.5
1.5–2.0	0.46	–	–	24.7 ± 0.9	14.4	10.6 ± 1.7
2.0–3.0	0.46	–	–	24.0 ± 1.1	12.1	12.3 ± 2.7
3.0–4.0	0.46	–	–	21.8 ± 0.9	14.5	7.5 ± 1.8
4.0–5.0	0.51	–	–	16.4 ± 0.7	14.6	1.9 ± 1.7
5.0–6.0	0.51	–	–	18.0 ± 0.4	13.6	4.5 ± 1.5
8.0–9.5	0.57	–	–	14.9 ± 0.7	13.5	1.4 ± 1.6
$\Sigma^{210}Pb_{xs}$ (dpm/cm^2)						30
Core SBC-6 (MANOP Site H: 6°35.0'N, 92°52.8'W)						
0.0–0.5	0.19	–	–	110 ± 11	39.0	75.1 ± 12.4
0.5–1.0	0.19	–	–	116 ± 10	37.8	82.7 ± 11.3
1.0–1.5	0.19	–	–	68.4 ± 6.2	36.5	33.7 ± 7.6
1.5–2.0	0.19	–	–	86.9 ± 10.8	38.7	51.0 ± 12.1
2.0–2.5	0.20	–	–	62.9 ± 4.8	43.6	20.5 ± 6.9
2.5–3.0	0.20	–	–	52.6 ± 2.0	35.8	17.9 ± 4.4
3.0–3.5	0.20	–	–	52.1 ± 2.8	34.7	18.5 ± 4.8
3.5–4.0	0.20	–	–	57.5 ± 4.8	37.5	21.1 ± 6.5
5.0–6.0	0.21	–	–	49.2 ± 3.4	41.8	7.8 ± 5.7
7.0–8.0	0.25	–	–	33.7 ± 2.9	36.3	−2.6 ± 4.9
$\Sigma^{210}Pb_{xs}$ (dpm/cm^2)						44
SBC-35 (MANOP Site S: 10°57.4'N, 140°5.2'W, 4938 m)						
0.0–1.0	0.28	–	–	57.5 ± 1.7	–	−12.7 ± 7.2 [g]
1.0–2.0	0.28	–	–	62.3 ± 2.0	–	−7.9 ± 7.3 [g]
2.0–3.0	0.29	–	–	74.6 ± 2.1	–	4.4 ± 7.3 [g]
3.0–4.0	0.30	–	–	72.3 ± 2.2	–	2.1 ± 7.3 [g]
4.0–5.0	0.30	–	–	96.3 ± 6.5	70.5	26.7 ± 9.6
5.0–6.0	0.36	–	–	81.9 ± 3.9	71.7	10.5 ± 8.3
6.0–7.0	0.36	–	–	66.0 ± 2.3	–	−4.2 ± 8.5 [g]
7.0–8.0	0.38	–	–	70.1 ± 4.9	–	−0.1 ± 8.5 [g]
8.0–9.0	0.38	–	–	72.5 ± 3.8	68.4	2.4 ± 8.2
$\Sigma^{210}Pb_{xs}$ (dpm/cm^2)						≤15
L3-3 (MANOP Site S: 11°0.7'N, 140°5.7'W, 4904 m)						
0.0–0.5	0.28	–	–	135 ± 5	45.9	91.4 ± 7.0
0.5–1.0	0.28	–	–	162 ± 7	44.6	120 ± 9
1.0–1.5	0.28	–	–	119 ± 4	53.2	67.5 ± 6.8
1.5–2.0	0.28	–	–	112 ± 5	56.6	57.2 ± 7.8
2.0–3.0	0.28	–	–	62.8 ± 2.9	46.2	17.0 ± 5.6
3.0–4.0	0.29	–	–	55.0 ± 2.7	–	5.8 ± 5.8 [g]
		–	–	51.0 ± 2.9	–	2.0 ± 5.8 [g]
4.0–5.0	0.30	–	–	47.2 ± 1.7	–	−2.1 ± 6.0 [g]
5.0–6.0	0.36	–	–	43.0 ± 2.0	–	−6.3 ± 5.5 [g]
		–	–	42.0 ± 2.0	–	−6.8 ± 5.1 [g]
6.0–7.0	0.36	–	–	37.3 ± 1.4	–	–
7.0–8.0	0.38	–	–	37.2 ± 1.5	–	–
8.0–9.0	0.38	–	–	30.4 ± 1.1	–	–
9.0–10.0	0.38	–	–	25.5 ± 0.9	–	–
$\Sigma^{210}Pb_{xs}$ (dpm/cm^2)						54

[a] Determined using gamma spectrometry. [b] Determined using radiochemical separation and alpha counting of ^{210}Po. [c] Determined using ^{222}Rn emanation. Uncertainty is 10% if not given. [d] Excess ^{210}Pb at core collection. Average of gamma and radiochemical measurements used for Nares cores. [e] Regional average used for core. [f] Average bulk density of KN54 BC52 used. [g] Average ^{226}Ra used to calculate excess ^{210}Pb. For Nares Abyssal Plain, average Ra for all samples > 3 cm (5.1 ± 1.2 dpm/g) used. For North Equatorial Pacific averages for respective cores are used.

References

1 M.K. Rama and E.D. Goldberg, Lead-210 in natural waters, Science 134, 98–99, 1961.

2 H. Craig, S. Krishnaswami and B.L.K. Somayajulu, Pb-210, Ra-226: Radioactive disequilibrium in the deep sea, Earth Planet. Sci. Lett. 17, 295–305, 1973.

3 M.P. Bacon, D.W. Spencer and P.G. Brewer, Pb-210/Ra-226 and Po-210/Pb-210 disequilibria in seawater and suspended particulate matter, Earth Planet. Sci. Lett. 32, 277–296, 1976.

4 D.W. Spencer, M.P. Bacon and P.G. Brewer, Models of the distribution of Pb-210 in a section across the North Equatorial Atlantic Ocean, J. Mar. Res. 39, 119–138, 1980a.

5 J.K. Cochran, M.P. Bacon, S. Krishnaswami and K.K. Turekian, Po-210 and Pb-210 distributions in the central and eastern Indian Ocean, Earth Planet Sci. Lett. 65, 433–452, 1983.

6 R. Carpenter, J.T. Bennett and M.L. Peterson, Pb-210 activities in and fluxes to sediments of the Washington continental slope and shelf, Geochim. Cosmochim. Acta. 45, 1155–1172, 1981.

7 W.S. Moore, K.W. Bruland and J. Michel, Fluxes of uranium and thorium series isotopes in the Santa Barbara Basin, Earth Planet. Sci. Lett. 53, 391–399, 1981.

8 Y. Nozaki, J.K. Cochran, K.K. Turekian and G. Keller, Radiocarbon and Pb-210 distribution in submersible deep-sea cores from Project FAMOUS, Earth Planet Sci. Lett. 34, 167–173, 1977.

9 T.-H. Peng, W.S. Broecker and W.H. Berger, Rates of benthic mixing in deep-sea sediments as determined by radioactive tracers, Quat. Res. 11, 141–149, 1979.

10 J.K. Cochran, Particle mixing rates in sediments of the eastern equatorial Pacific: Evidence from Pb-210, Pu-239,240 and Cs-137 distributions at MANOP sites, Geochim. Cosmochim. Acta. 49, 1195–1210, 1985.

11 M.C. Stordal, J.W. Johnson, N.L. Guinasso, Jr. and D.R. Schink, Quantitative evaluation of bioturbation rates in deep ocean sediments II, Comparison of rates determined by Pb-210 and Pu-239,240, Mar. Chem. 17, 99–114, 1985.

12 D.J. DeMaster and J.K. Cochran, Particle mixing rates in deep-sea sediments determined from excess Pb-210 and Si-32 profiles, Earth Planet. Sci. Lett. 61, 257–271, 1982.

13 D.J. DeMaster, B.A. McKee, C.A. Nittrouer, D.C. Brewster and P.E. Biscaye, Rates of sediment reworking at the HEBBLE site based on measurements of Th-234, Cs-137 and Pb-210, Mar. Geol. 66, 133–148, 1985.

14 J.N. Smith, B.P. Boudreau and V. Noshkin, Plutonium and Pb-210 distributions in northeast Atlantic sediments: subsurface anomalies caused by non-local mixing, Earth Planet. Sci. Lett. 81, 15–28, 1986/87.

15 P. Kershaw, C-14 and Pb-210 in NE Atlantic sediments: evidence of biological reworking in the context of radioactive waste disposal, J. Environ. Radioact. 2, 115–134, 1985.

16 Y. Nozaki, Ra-226–Rn-222–Pb-210 systematics in seawater near the bottom of the Ocean, Earth Planet. Sci. Lett. 80, 36–40, 1986.

17 J.K. Cochran, H.D. Livingston, D.J. Hirschberg and L.D. Surprenant, Natural and anthropogenic radionuclide distributions in the Northwest Atlantic Ocean, Earth Planet. Sci. Lett. 84, 135–152, 1987.

18 N.H. Cutshall, I.L. Larsen and C.R. Olsen, Direct analysis of Pb-210 in sediment samples: Self absorption corrections, Nucl. Inst. Meth. 206, 309–312, 1983.

19 I. Walsh, J. Dymond and R. Collier, Rates of recycling of biogenic components of settling particles in the ocean derived from sediment trap experiments, Deep-Sea Res. 35, 43–58, 1988.

20 H.G. Ostlund, H. Craig, W.S. Broecker and D. Spencer, GEOSECS Atlantic, Pacific and Indian Ocean Expeditions, Vol. 7 Shorebased Data and Graphics, 200 pp., U.S. Gov. Print. Off., Washington, D.C., 1987.

21 Y. Chung and H. Craig, Pb-210 in the Pacific: the GEOSECS measurements of particulate and dissolved concentrations, Earth Planet. Sci. Lett. 65, 406–432, 1983.

22 Y. Nozaki, K.K. Turekian, and K. Von Damm, Pb-210 in GEOSECS water profiles from the North Pacific, Earth Planet Sci. Lett. 49, 393–400, 1980.

23 Y. Chung, R. Finkel, M.P. Bacon, J.K. Cochran and S. Krishnaswami, Intercomparison of Pb-210 measurements at GEOSECS station 500 in the northeast Pacific, Earth Planet. Sci. Lett. 65, 393–405, 1983.

24 M.P. Bacon, D.W. Spencer and P.G. Brewer, Lead-210 and Polonium-210 as marine geochemical tracers: review and discussion of results from the Labrador Sea, in: Natural Radiation Environment III, T.F. Gesell and W.F. Lowder, eds., Vol. 1, U.S. DOE Rep. CONF-780422, pp 473–501, 1980.

25 D.W. Spencer, M.P. Bacon and P.G. Brewer, The distribution of Pb-210 and Po-210 in the North Sea, Thalassia Jugosl. 16, 125–154, 1980b.

26 Y. Nozaki, J. Thomson and K.K. Turekian, The distribution of Pb-210 and Po-210 in surface waters of the Pacific Ocean, Earth Planet. Sci. Lett. 32, 304–312, 1976.

27 K.K. Turekian, Y. Nozaki and L.K. Benninger, Geochemistry of atmospheric radon and radon products, Annu. Rev. Earth Planet. Sci. 5, 227–255, 1977.

28 K.K. Turekian, L.K. Benninger and E.P. Dion, Be-7 and Pb-210 total deposition fluxes at New Haven, Connecticut and at Bermuda, J. Geophys. Res. 88, 5411–5415, 1983.

29 K.K. Turekian, W.C. Graustein and J.K. Cochran, Lead-210 in the SEAREX Program. An aerosol tracer across the Pacific, in: Chemical Oceanography, J.P. Riley, R. Chester, R. Duce eds., Academic Press, New York, N.Y., Vol. 10, pp. 51–81, 1989.

30 M. Lyle and J. Dymond, Metal accumulation rates in the Southeast Pacific-errors introduced from assumed bulk densities, Earth Planet. Sci. Lett. 30, 164–168, 1976.

31 E.A. Boyle, S.D. Chapnick, G.T. Shen and M.P. Bacon, Temporal variability of lead in the western North Atlantic Ocean, J. Geophys. Res. 91, 8573–8593, 1986.

32 N.S. Fisher, J.K. Cochran, S. Krishnaswami and H.D. Livingston, Predicting the oceanic flux of radionuclides on sinking biogenic debris, Nature 355, 622–625, 1988.

33 W.S. Moore and J. Dymond, Correlation of Pb-210 removal with organic carbon fluxes in the Pacific Ocean, Nature 331, 339–341, 1988.

34 M.P. Bacon and R.F. Anderson, Distribution of thorium

isotopes between dissolved and particulate forms in the deep sea, J. Geophys. Res. 87, 2045–2056, 1982.
35 G.G. Mathieu, P.E. Biscaye, R.A. Lupton and D.E. Hammond, System for measurement of Rn-222 at low levels in natural waters, Health Phys. 55, 989–992, 1988.
36 J.K. Cochran and S. Krishnaswami, Radium, thorium, uranium and Pb-210 in deep-sea sediments and sediment pore waters from the North Equatorial Pacific, Am. J. Sci. 280, 849–889, 1980.
37 J.Y. Aller, Quantifying sediment disturbance by bottom currents and its effect on benthic communities in a deep-sea western boundary zone. Deep-Sea Res. 36, 901–934, 1989.
38 D.J. DeMaster, D.C. Brewster, B.A. McKee and C.A. Nittrouer, Rates of particle scavenging, sediment reworking and longitudinal ripple formation at the HEBBLE site based on measurements of Th-234 and Pb-210, Deep-Sea Res. (in press).
39 O.J. Koblentz-Mishke, V.V. Volkovinsky and J.G. Kabanova, Plankton primary production of the world ocean. Scientific Exploration of the South Pacific, W. Wooster, ed., Nat. Acad. Sci., pp 183–193, 1970.
40 R.W. Eppley and B.J. Peterson, Particulate organic matter flux and planktonic new production in the deep ocean, Nature 282, 677–680, 1979.
41 J.H. Martin, G.A. Knauer, D.M. Karl and W.W. Broenkow, VERTEX: Carbon cycling in the northeast Pacific, Deep-Sea Res. 34, 267–285, 1987.
42 F.P. Chavez and R.T. Barber, An estimate of new production in the equatorial Pacific, Deep-Sea Res. 34, 1229–1243, 1987.
43 W.E. Esaias, G.C. Feldman, C.R. McClain and J.A. Elrod, Monthly-satellite-derived phytoplankton pigment distribution for the North Atlantic Ocean basin, EOS, Trans. Am. Geophys. Union 67, 835–837, 1986.
44 K.O. Buesseler, H.D. Livingston and E.R. Sholkovitz, Pu-239,240 and excess Pb-210 inventories along the shelf and slope of the northeast U.S.A., Earth Planet. Sci. Lett. 76, 10–22, 1985/86.
45 M.P. Bacon, R.A. Belastock, M. Tecotzky, K.K. Turekian and D.W. Spencer, Lead-210 and polonium-210 in ocean water profiles of the continental shelf and slope south of New England, Cont. Shelf Res. 8, 841–853, 1988.
46 W.Q. Li, N.L. Guinasso, Jr., K.H. Cole, M.D. Richardson, J.W. Johnson and D.R. Schink, Radionuclides as indicators of sedimentary processes in abyssal Caribbean sediments, Mar. Geol. 68, 187–204, 1985.
47 J.N. Smith and C.T. Schafer, Bioturbation processes in continental slope and rise sediments delineated by Pb-210, microfossil and textural indicators, J. Mar. Res. 42, 1117–1145, 1984.
48 J. Thomson and K.K. Turekian, Po-210 and Pb-210 distributions in ocean water profiles from the eastern South Pacific, Earth Planet. Sci. Lett. 32, 297–303, 1976.
49 R.M. Key, J.L. Sarmiento and W.S. Moore, Distribution of Ra-228 and Ra-226 in the Atlantic Ocean. Tech. Rep. #85-1, TTO Test Cruise and TTO NAS Legs 1–3, 78 pp., 1985.
50 R.A. Jahnke, S.R. Emerson, J.K. Cochran and D.J. Hirschberg, Fine scale distributions of porosity and particulate excess Pb-210, organic carbon and $CaCO_3$ in surface sediments of the deep equatorial Pacific, Earth Planet. Sci. Lett. 77, 59–69, 1986.
51 R.C. Aller and D.J. DeMaster, Estimates of particle flux and reworking at the deep-sea floor using Th-234/U-238 disequilibrium, Earth Planet. Sci. Lett. 67, 308–318, 1984.
52 H.-S. Yang, Y. Nozaki, H. Sakai, Y. Nagaya and K. Nakamura, Natural and man-made radionuclide distributions in Northwest Pacific deep-sea sediments: rates of sedimentation, Bioturbation and Ra-226 migration, Geochim. J. 20, 29–40, 1986.
53 B.L.K. Somayajulu, P. Sharma and W.H. Berger, Be-10, C-14 and U-Th decay series nuclides and $\delta^{18}O$ in a box core from the central North Atlantic, Mar. Geol. 54, 169–180, 1984.
54 J. Thomson, S. Colley and P.P.E. Weaver, Bioturbation into a recently emplaced deep-sea turbidite surface as revealed by $^{210}Pb_{xs}$, $^{230}Th_{xs}$ and planktonic foraminifera distributions, Earth Planet. Sci. Lett. 157–171, 1988.